International Journal of Engineering Science Invention (IJESI)
ISSN (Online): 2319-6734, ISSN (Print): 2319-6726
www.ijesi.org ||Volume 9 Issue 9 Series I || September 2020 || PP 41-55

Role of Magnetic Field with Nonlinear Thermal Radiation and Ohmicdissipation of a Casson Nanofluid over Stretching Sheet Considering Slip Velocity

Netai Roy
Department of Mathematics, Surendranath College, Kolkata-700009, West Bengal, India

Abstract: *The present study analyses the combined effects of non-linear thermal radiation and velocity slip in the boundary layer flow over stretching surface of a Casson nanofluid considering the effect of magnetic field and Brownian motion. A system of nonlinear ordinary differential equations is obtained here after applying the similarity transformation on the boundary layer basic equations and solved them numerically using Runge-Kutta-Fehlberg fifth-order method with shooting tech- nique. The Prandtl number, magnetic parameter, slip factor, Brownian motion parameter, Lewis number, thermal radiation parameter, Casson fluid parameter and thermophoresis parameters play the key role in the Casson nanofluid flow, heat and mass transfer. The effect of various important physical parameters on the local Nusselt and local Sherwood numbers is addressed in this study. In the study, it is observed that local Nusselt number reduces with augmentation in the value of the Brownian motion parameter, thermophoretic parameter and radiation parameter. Results confirm that conduction form increases with rise of magnetic parameter. Enhancement of slip velocity boosts the temperature profile and the influence of Casson parameter be suited to rise concentration profile.*

Keywords: *Brownian motion, Casson nanofluids, magnetic parameter, similarity transformation, slip factor, thermal radiation, thermophoresis.*

Date of Submission: 30-08-2020 Date of Acceptance: 15-09-2020

Nomenclature

b	Constant related to stretching sheet velocity
C	Casson nanoparticle volume fraction
Cf_x	Skin fraction coefficient
C_w	Casson nanoparticle volume fraction at the wall
C_∞	Free stream Casson nanoparticle volume fraction
D_B	Brownian diffusion coefficient
D_T	Thermophoretic diffusion coefficient
N^*	Slip constant
p	Fluid pressure
p_y	Yield stress of the non-Newtonian fluid
s	Suction parameter
T	Temperature of the nanofluid
T_∞	Free stream temperature
T_w	Temperature at the wall
u	Velocity component in x-direction
u_w	Stretching sheet velocity
U	Free stream velocity of the nanofluid
v	Velocity component in y-direction
x, y	Direction along and perpendicular to the plate, respectively

Greek symbols

α	Fluid thermal diffusivity
γ	Casson fluid parameter
η	Similarity variable
θ	Dimensionless temperature of the fluid
κ	Coefficient of thermal conductivity
κ^*	Mean absorption coefficient
λ	Dimensionless slip factor

μ_B	Plastic dynamic viscosity of the non-Newtonian fluid
μ_f	Dynamic viscosity of the fluid
ν	Kinematic viscosity of the fluid
π_c	Critical value of the product based on the non-Newtonian model
ρ_f	Density of the Casson nanofluid
ρ_p	Casson nanoparticle mass density
$(\rho c)_f$	Heat capacity of the fluid
$(\rho c)_p$	Effective heat capacity of the nanoparticle material
σ^*	Stefan-Boltzmann constant
τ	Parameter defined by ratio between $(\rho c)_p$ and $(\rho c)_f$
ϕ	Solid volume fraction of the Casson nanoparticles
ψ	Dimensional stream function
Superscripts	
$'$	Differentiation with respect to y
Subscripts	
f	Fluid
S	Solid

I. Introduction

Now a days, the usage of biological fluids as printer inks, multi-grade oils, lubricating greases, gypsum pastes, ceramics, paints, fruit juices, polymers, liquid detergents, blood etc. in industrial manufacturing process change the flow characteristic considering stress during viscos- ity and in this way deflect from the classical Newtons law of viscosity. In this situation, many researchers proposed and introduced several models of non-Newtonian fluids based on their mul- tiple flow characteristics. Casson fluid is one of such indicative non-Newtonian fluid which is envisaged to reflect the shear thinning characteristic. When the shear stress rises to a level nu- merous higher than the produced stress, Casson fluid acts like a Newtonian fluid. Casson first time indicated and predict the flow character of pigment-oil suspensions of printing ink. Cas- son fluid is considered for suitable rheological data better than general viscoplastic models for different fluids. When the shear stress is the smaller comparison to the produced stress then Casson fluid behaves like solid and in case shear stress turns greater than the produced stress when it starts to deform. Nanofluid is defined to be a fluid, produced by a suspension of solid nanometer-sized particles (1-100 nm), termed as nanoparticles in base fluid. Metals, oxides, carbides or carbon nanotubes are the main components of nanoparticles. These nanoparticles increases thermal conductivity and the convective heat transfer coefficient effectively of the base fluid [1]. In industrial uses, cooling of a metal or glass sheet, thermal radiation play an important role. The thermal conductivity of these fluids gets into the heat transfer between the fluid and heating surface. Choi [2] first time employed a momentous technique to mix the nanoparticles in the base liquid which exposed enhancement in the thermal conductivity of the fluid up to two times on an average. In recent time the industrial revolution is more influenced by considerable application of nanotechnology. The exploration on various viscosities of nanofluids and flourish- ing the model on thermal conductivity have been carried out by numerous researchers over the past decade. Kuznetsav and Nield [3] showed the existence of nanoparticles on natural convec- tion boundary layer flow past a vertical sheet in their studies. Makinde and Aziz [4] studied the boundary layer flow of a nanofluid towards a stretching surface considering convective boundary condition. Influence of thermal radiation and slip velocity on heat transfer in nanofluid over a stretching sheet is examined by Pal and Roy [5]. Investigations on Casson nanofluid considering boundary layer flow using different ge- ometries have been performed in a large scale during the last few years. The role of thermal radiation on Casson fluid flow and heat transfer behavior with suction/blowing along an unsteady stretching surface was considered by Mukhopadhyay [6]. The flow natures of a Casson fluid in porous medium along with thermal radiation over an exponentially stretching sheet studied by Pramanik [7]. He concluded that an increment in the value of the Casson parameter decrease the velocity field. The steady magnetohydrodynamic heat and mass transfer of a Casson nanofluid towards a vertical stretching surface considering the effects of thermal radiation and Brownian motion was investigated by Pal et al. [8]. Sarojamma et al. [9] studied the effects of heat and mass transfer of the MHD Casson fluid flow in a vertical channel. They showed the flow behaviors of Casson fluid towards the stretching walls in parallel channel considering heat and mass transfer characteristics with a uniform transverse magnetic field. The effects of thermal radiation shows a momentous role in space technology, high temperature processes and regulating heat transfer in polymer processing industry for the excellence of the final product depends mainly on the heat regulating factors. The radiative effects on boundary layer flow considering different phenom- ena were studied

by many investigators. Bhattacharyya [10] considered the impact of thermal radiation and heat transfer of Casson fluid over a stretching sheet with a two-dimensional mag.

netohydrodynamic flow. Oyelakin et al. [11] investigated the flow characteristic of an unsteady Casson nanofluid over a stretching sheet with the Dufour and Soret effects. The magnetohydrodynamic boundary layer flow and heat transfer of Casson nanofluid over an exponentially stretching surface was studied by Mukhopadhyay et al. [12].

But so far, no attempt has been made to study the effect of magnetic energy with velocity slip boundary condition on the heat and mass transfer characteristics of Casson nanofluid flow over a stretching sheet in the presence of non-linear thermal radiation and Ohmic dissipation. Thus the aim of this paper is to study the effect of velocity slip boundary condition on heat and mass transfer characteristics of Casson nanofluid flow over a stretching sheet in the presence of Ohmic dissipation, thermal radiation and the influence of magnetic field. The governing equations are explored numerically using Runge-Kutta-Fehlberg method with shooting techniques.

2. Formulation of the Problem

A two-dimensional flow of an incompressible Casson nanofluid over a stretching surface is taken into account . The well known rheological equation of state is as follows [16]:

$$\tau_{ij} = \begin{cases} 2(\mu_B + \frac{p_y}{\sqrt{2\pi}})e_{ij}, & \pi > \pi_c, \\ 2(\mu_B + \frac{p_y}{\sqrt{2\pi_c}})e_{ij}, & \pi < \pi_c, \end{cases}$$

where the (i, j)-th component of the stress tensor is τ_{ij}, $\pi = e_{ij}e_{ij}$ and e_{ij} are the (i, j)-th component of the deformation rate. Consider a coordinate frame so that the x-axis is aligned vertically upwards and vertical plate at y = 0 (Fig. 1). Here, $U(x) = bx$ is considered as velocity of

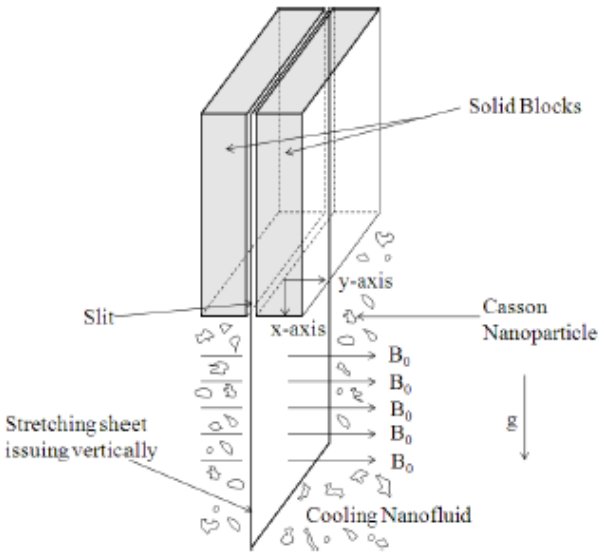

Figure 1: Flow configuration.

the stretching sheet with b as a constant. The coordinate x is measured towards the stretching surface. The geometry of the problem is displayed in Fig. 1. A uniform magnetic field of strength B_0 with a non-linear thermal radiation is employed Parallel to y-axis. The wall temperature T_w and the nanoparticle volume fraction C_w are taken to be constants at the stretching surface and also

as y tends to infinity, the bounded value of the temperature and nanoparticle volume fraction is considering to be a constant T_∞ and C_∞, respectively. The equations of conservation of momentum, thermal energy and Casson nanoparticles concentration in Cartesian coordinates system, considering the dynamic effects of Casson nanoparticles with Ohmic dissipation, velocity slip boundary condition and the magnetic field are written as follows

$$\frac{\partial u}{\partial x}+\frac{\partial v}{\partial y}=0, \tag{1}$$

$$u\frac{\partial u}{\partial x}+v\frac{\partial u}{\partial y}=-\frac{1}{\rho_f}\frac{\partial p}{\partial x}+\left(1+\frac{1}{\gamma}\right)\frac{\mu_f}{\rho_f}\left(\frac{\partial^2 u}{\partial x^2}+\frac{\partial^2 u}{\partial y^2}\right)-\frac{\sigma B_0^2}{\rho_f}u, \tag{2}$$

$$u\frac{\partial T}{\partial x}+v\frac{\partial T}{\partial y}=\alpha\left(\frac{\partial^2 T}{\partial x^2}+\frac{\partial^2 T}{\partial y^2}\right)-\frac{1}{(\rho c_p)_f}\frac{\partial q_r}{\partial y}-\frac{\sigma B_0^2}{(\rho c_p)_f}u^2$$
$$+\tau\left[D_B\left(\frac{\partial C}{\partial x}\frac{\partial T}{\partial x}+\frac{\partial C}{\partial y}\frac{\partial T}{\partial y}\right)+\frac{D_T}{T_\infty}\left(\left(\frac{\partial T}{\partial x}\right)^2+\left(\frac{\partial T}{\partial y}\right)^2\right)\right], \tag{3}$$

$$u\frac{\partial C}{\partial x}+v\frac{\partial C}{\partial y}=D_B\left(\frac{\partial^2 C}{\partial x^2}+\frac{\partial^2 C}{\partial y^2}\right)+\left(\frac{D_T}{T_\infty}\right)\left(\frac{\partial^2 T}{\partial x^2}+\frac{\partial^2 T}{\partial y^2}\right). \tag{4}$$

The associated boundary conditions are

$$u=U_w(x)+U_s,\quad v=v_0,\quad C=C_w,\quad T=T_w,\ \ at\ \ y=0,$$
$$u=0,\quad v=0,\quad C=C_\infty,\quad T=T_\infty,\quad as\ \ y\to\infty. \tag{5}$$

where, $\gamma=\frac{\sqrt{2\pi_c}\mu_B}{p_y}$ is the Casson parameter, $\tau=\frac{(\rho c)_p}{(\rho c)_f}$, which is the ratio between the effective heat capacity of the nanoparticle material and heat capacity of the fluid.

The other terms are given in the nomenclature with their usual meanings.

Dimensionless variables and the stream function can be taken taken in the following form

$$\psi=(b\nu)^{1/2}xf(\eta),\qquad \eta=\left(\frac{D}{\nu}\right)^{1/2}y, \tag{6}$$

$$\theta(\eta)=\frac{T-T_\infty}{T_w-T_\infty},\qquad \phi(\eta)=\frac{C-C_\infty}{C_w-C_\infty}. \tag{7}$$

Now considering velocities $v=-\frac{\partial\psi}{\partial x}, u=\frac{\partial\psi}{\partial y}$, then Eq. (1) is gratified identically. Since the pressure gradient is considered as negligible so the flow takes place only due to the stretching sheet and the pressure out side the boundary layer is constant. The Rosseland approximation [16] gives the radiative heat flux term q_r in eq. (3) of the form, $q_r=-\frac{4\sigma^*}{3k^*}\frac{\partial T^4}{\partial y}$. T^4 may be written as $T^4=T_\infty^4[1+(\theta_w-1)\theta]^4$, where, $\theta_w=\frac{T_w}{T_\infty}$ is the wall temperature excess ratio parameter.

The application of similarity transformations (6) & (7) on the governing Eqs. (2)-(4), we have

$$f'''+\frac{\gamma}{1+\gamma}[ff''-f'^2-Mf']=0, \tag{8}$$

$$[(1+\frac{4}{3}Rd\,[1+(\theta_w-1)\theta]^3)\theta']'+Pr(f\theta'+Nb\theta'\,\phi'+Nt\,\theta'^2-E_c\,M\,f'^2)=0, \tag{9}$$

$$\phi'' + Le\, f\phi' + \frac{Nt}{Nb}\theta' = 0. \tag{10}$$

By using the Navier slip condition and the boundary layer approximations we have,

$$u - U_w(x) = N^*\rho\nu\frac{\partial u}{\partial y} = U_S, \tag{11}$$

Now Eq. (11) reduced to the following form after applying the similarity transforms

$$f'(0) - \lambda f''(0) - 1 = 0. \tag{12}$$

Boundary condition (5) now becomes by using (7), (12) & (13) as

At $\eta = 0$:

$$f = s, \quad f' = 1 + \lambda f'', \quad \phi = 1, \quad \theta = 1. \tag{13}$$

At $\eta \to \infty$:

$$f' = 0, \quad \phi = 0, \quad \theta = 0, \tag{14}$$

where

$$Pr = \frac{\nu}{\alpha}, \quad Le = \frac{\nu}{D_B}, \quad Nt = \frac{\tau}{\nu}\frac{D_T}{T_\infty}\Delta\theta, \quad Nb = \frac{\tau D_B\Delta\phi}{\nu},$$

$$M = \sqrt{\frac{\sigma B_0^2 U}{c\rho_f}}, \quad Rd = \frac{\kappa\kappa^*}{4\sigma_1 {T_\infty}^3}, \quad E_c = \frac{U_w^2}{\Delta\theta C_p}. \tag{15}$$

are the Prandtl number, the Lewis number, the thermophoresis parameter, the Brownian motion parameter, the magnetic parameter, the Radiation parameter and the Eckert number respectively.

For nanofluids, the assumption of without slip is no longer holds and an absolute degree of tangential slip must be allowed, since Casson nanofluid flow commonly exhibits partial slip contrary to solid surface, which can be differentiated by the slip length [14].

The essential parameters, such as local Nusselt number (Nu_x) and Sherwood number (Sh_x) are obtained as

$$Nu_x = \frac{xq_w}{\kappa(T_w - T_\infty)}, \quad Sh_x = \frac{xq_m}{D_B(\phi_w - \phi_\infty)}, \tag{16}$$

Considering wall temperature gradient q_w and concentration gradients q_m, are as follow

$$q_w = -\kappa\sqrt{\frac{b}{\nu}}(T_w - T_\infty)(1 + \frac{4}{3Rd}{\theta_w}^3)\theta'(0). \tag{17}$$

and

$$q_m = D_B\sqrt{\frac{b}{\nu}}(C_w - C_\infty)\phi'(0). \tag{18}$$

From eq. (16) the following results are obtained after using the Eqns. (17) & (18)

$${Re_x}^{-\frac{1}{2}}Nu_x = -(1 + \frac{4}{3Rd}{\theta_w}^3)\theta'(0), \quad {Re_x}^{-\frac{1}{2}}Sh_x = -\phi'(0), \tag{19}$$

considering $Re_x = u_w(x)x/\nu$ is the local Reynolds number. ${Re_x}^{-\frac{1}{2}}Nu_x$ and ${Re_x}^{-\frac{1}{2}}Sh_x$ are taken as the values of reduced Nusselt number and the reduced Sherwood number respectively.

3. Methodology

From the highly nonlinear system of equations (8)- (10) one can't be able to obtain solutions analytically and therefore it is better to solve them numerically. The system of modified Eqs. (8)- (10) and the boundary conditions (13) and (14) simultaneously are more systematically solved by using Runge-Kutta-Fehlberg method with shooting techniques by systematical guessing the values of $f''(0), \theta'(0)$ and $\phi'(0)$. At the very early step, the higher order non-linear differential equation (8) - (10) are transformed into simultaneous differential equations of first order. The governing non-linear ordinary differential equations which are transformed to a set of simultaneous first order differential equations are shown in the following,

$$y_1 = f,\ y_2 = f',\ y_3 = f'',\ y_4 = \theta,\ y_5 = \theta',\ y_6 = \phi,\ y_7 = \phi', \tag{20}$$

$$F_1 = y_2,\ F_2 = y_3,\ F_3 = \frac{\gamma}{1+\gamma}[y_2{}^2 - y_1 y_3 + M y_2], F_4 = y_5,$$

$$F_5 = -\frac{3}{3Rd + 4\{1 + (\theta_w - 1)\, y_4\}^3}[Rd\ Pr\ (y_1 y_5 + Nb\, y_5 y_7 + Nt\, y_5{}^2 - Ec\, M y_2{}^2)$$

$$+4\,(\theta_w - 1)\, y_5{}^2\{1 + (\theta_w - 1)\, y_4\}^2],\ F_6 = y_7,$$

$$F_7 = -\left[Le\, y_1\, y_7 + \frac{Nt}{Nb} F_5\right]. \tag{21}$$

The boundary condition becomes

$$y_1 = s,\ y_2 = 1 + \lambda y_3,\ y_4 = 1,\ y_6 = 1\ at\ \eta = 0,$$

$$y_2 = 0,\ y_4 = 0,\ y_6 = 0,\ as\ \eta \to \infty. \tag{22}$$

4. Results and Discussion

Applying Runge-Kutta-Fehlberg method with shooting techniques, eqs. (20)-(21) considering the boundary conditions (22) have been solved numerically for several values of the governing parameters $Pr, s, Le, \lambda, Rd, Ec, Nb, Nt, \gamma$ and θ_w. Neglecting the effects of $Nb, Nt, Rd, M, s, Ec, \lambda$ and Casson parameter γ, the outcomes for the reduced Nusselt number $-\theta'(0)$ are compared with those acquired by Kandasamy et al. [15], Wang [16], and Gorla and Sidawi [17] for several values of Pr in Table 1. We observed that the comparison indicates an excellent similarity for several values of the physical parameters. Therefore, we are doubtless that the current results are strongly immaculate.

In Table 2, the values of the reduced Nusselt number and reduced Sherwood number are calculated for different inputs of the slip factor λ, suction parameter s, Casson parameter γ and Eckert number Ec for $Le = 10.0$, $Pr = 2.0$, $M = 0.5$, $Rd = 5.0$, $Nt = 0.5$ and $\theta_w = 0.5$. It is clearly seen that an increment in the values of the suction parameter s there is a rise in the value of the reduced Nusselt number and reduced Sherwood number, but the opposite trend is observed by rising the value of the Casson parameter γ and slip factor λ. It is also displayed in the table that an enhancement in the value of the Eckert number there is an advancement in the reduced Nusselt number and an opposite effect is obtained on the values of the reduced Sherwood number.

Table 1: Comparison of the present results for reduced Nusselt number $-\theta'(0)$ with Kandasamy et al. [15], Wang [16], Gorla and Sidawi [17].

Pr	Kandasamy *et al.*[15]	Wang [16]	Gorla and Sidawi [17]	Present work
0.07	0.066129	0.0656	0.0656	0.066496396
0.20	0.169136	0.1691	0.1691	0.169089453
0.70	0.454285	0.4539	0.5349	0.453916162
2.00	0.911423	0.9113	0.9113	0.911357683
7.00	1.895264	1.8954	1.8905	1.895403320
20.00	3.353853	3.3539	3.3539	3.353904140
70.00	6.462189	6.4622	6.4622	6.462199530

The values of the reduced Sherwood number and reduced Nusselt number are also calculated for different values of the thermophoresis parameter Nt, the magnetic parameter M, the radiation parameter Rd and the wall temperature excess ratio θ_w for $Le = 10.0$, $\gamma = 1.0$, $Pr = 2.0$, $\lambda = 0.5$, $s = 0.5$, $Nb = 0.5$, $Ec = 0.1$, in Table 3. It is seen from this table that an enhancement in the values of M, Nt and θ_w there is a fall in the values of the reduced Nusselt number but the opposite trend is observed by increasing the value of Rd. It is also exhibited in the table that an advancement in the value of M there is a reduction in the values of reduced Sherwood number.

The variation of velocity profiles $f'(\eta)$ for different values of the Casson parameter γ, the mag-

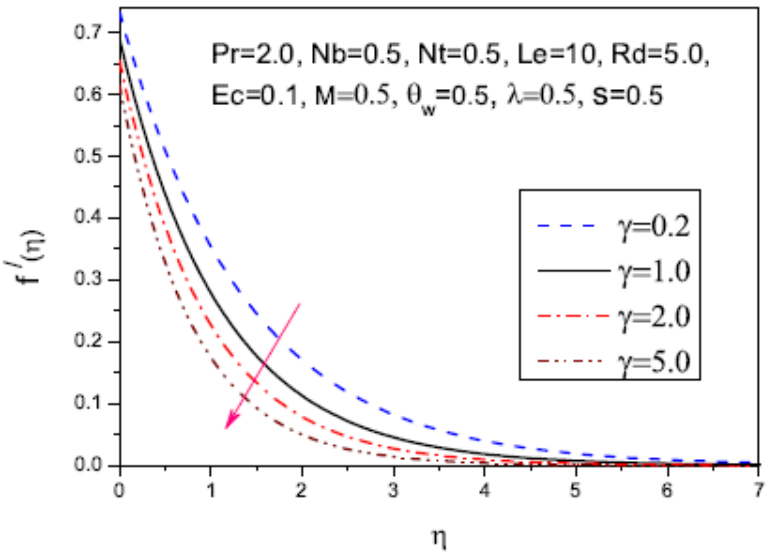

Figure 2: Velocity distribution $f'(\eta)$ vs. η for several values of Casson fluid parameter γ.

netic parameter M, the suction parameter s and the slip parameter λ in the momentum boundary

Table 2: Effects of λ, s, γ and Ec on the Nusselt number $-\theta'(0)$ and Sherwood number $-\phi'(0)$ when $Le = 10.0$, $Pr = 2.0$, $Rd = 5.0, \theta_w = 0.5$, $Nb = 0.5$, $Nt = 0.5$ and $M = 0.5$.

λ	s	γ	Ec	$-\theta'(0)$	$-\phi'(0)$
0.50	0.50	1.00	0.10	0.43514771	8.3170508
1.00				0.40512338	8.2178885
2.00				0.37162008	8.1098961
2.50				0.36090228	8.0761429
0.50	0.25	1.00	0.10	0.32650132	6.5565993
	1.00			0.67711796	12.2322790
	1.50			0.93950426	16.4185880
	2.00			1.21319040	20.7484450
	0.50	0.20	0.10	0.48244021	8.4192844
		1.00		0.43514771	8.3170508
		3.00		0.41383620	8.2702622
		10.00		0.40307664	8.2463470
		∞		0.39761806	8.2341088
		1.00	0.01	0.42696241	8.3199042
			0.05	0.43060266	8.3186352
			0.10	0.43514771	8.3170508
			0.50	0.47130080	8.3044560
			1.00	0.51598581	8.2889063

layer are exhibited in Figs. 2, 3, 4 & 5 respectively for $Pr = 2.0$, $Le = 10.0$, $\theta_w = 0.5$, $Nb = 0.5$, $Ec = 0.1$, $Nt = 0.5$, $Rd = 5.0$. From fig. 2, 3 & 4 it is observed that velocity profiles decreases with the increment in the values of γ, M and s for the fall of the momentum boundary layer thickness due to an enhancement in the Casson parameter, the magnetic parameter and the suction parameter. From Fig. 5 it is also observed that by increasing the slip factor λ there is a fall in the lateral velocity close to the stretching surface.

The effects of the magnetic parameter M, the thermophoretic parameter Nt, the slip parameter λ, the Brownian motion parameter Nb, the radiation parameter Rd and the suction parameter s on the temperature profiles against η are depicted in the figs. 6 - 11. It is noticed from figs. 6- 9 that the effect of an augmentation in the magnetic parameter, the thermophoretic parameter, the slip parameter and the Brownian motion parameter is to enhance the value of the temperature $\theta(\eta)$ absolutely the thermal boundary layer respectively.

Figs. 10 & 11 display that the effect due to a rise in the radiation parameter and the suction parameter number is to downfall the value of the temperature $\theta(\eta)$ fully the thermal boundary layer respectively. Due to the suction for all value of s, the fluid is arrived nearer to the stretching surface which motivates the reduction of thermal boundary layer thickness. The raise in the radiation parameter signifies the remission of heat energy from the flow region, and the fluid temperature reduces as the thermal boundary layer thickness turns thicker.

Table 3: Effects of Nt, M, Rd and θ_w on the Nusselt number $-\theta'(0)$ and the Sherwood number $-\phi'(0)$ when $Le = 10.0$, $Pr = 2.0$, $\lambda = 0.5$, $Ec = 0.1$, $Nb = 0.5$, $\gamma = 1.0$, and $s = 0.5$.

Nt	M	Rd	θ_w	$-\theta'(0)$	$-\phi'(0)$
0.10	0.50	5.00	0.50	0.60411157	8.1084025
1.00				0.30363326	8.5662653
2.00				0.17342784	8.8494813
2.50				0.14025479	8.9059756
0.50	0.10	5.00	0.50	0.44035599	8.3496176
	1.00			0.42937855	8.2845225
	2.00			0.41979556	8.2354458
	3.00			0.41210479	8.1988967
	0.50	0.50	0.50	0.52345216	8.1671579
		1.00		0.48729863	8.2384900
		5.00		0.43514771	8.3170508
		10.00		0.42657236	8.3283369
		5.00	0.10	0.42447462	8.3355080
			0.50	0.43514771	8.3170508
			1.00	0.44334507	8.2679054
			2.00	0.34319649	8.1694332
			3.00	0.19839157	8.1092352

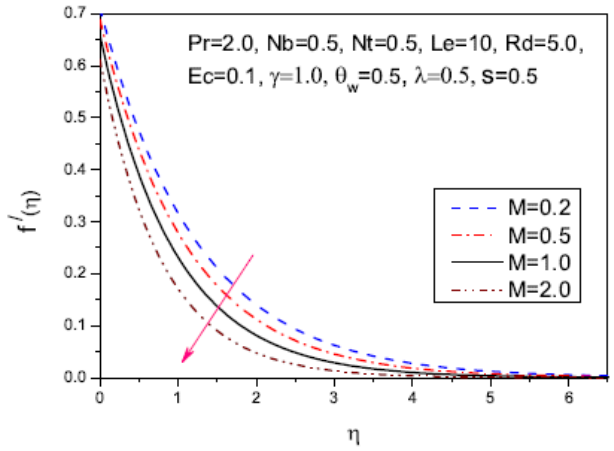

Figure 3: Velocity distribution $f'(\eta)$ vs. η for several values of Magnetic parameter M.

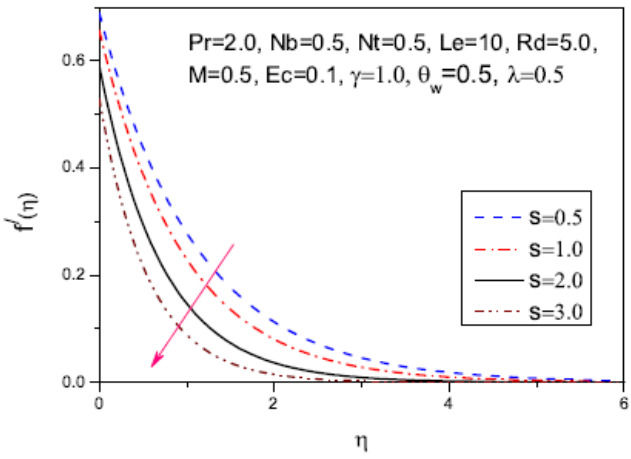

Figure 4: Velocity distribution $f'(\eta)$ vs. η for several values of suction parameter s.

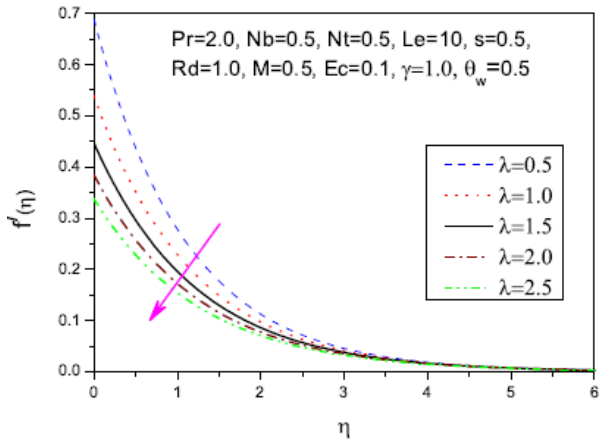

Figure 5: Velocity distribution $f'(\eta)$ vs. η for several values of slip factor λ.

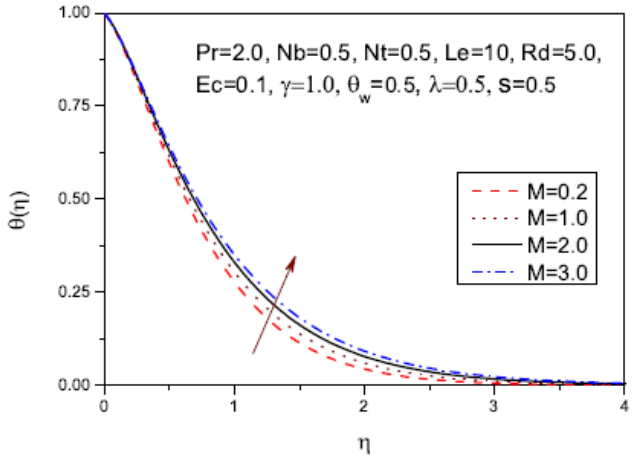

Figure 6: Temperature distribution $\theta(\eta)$ vs. η for several values of M.

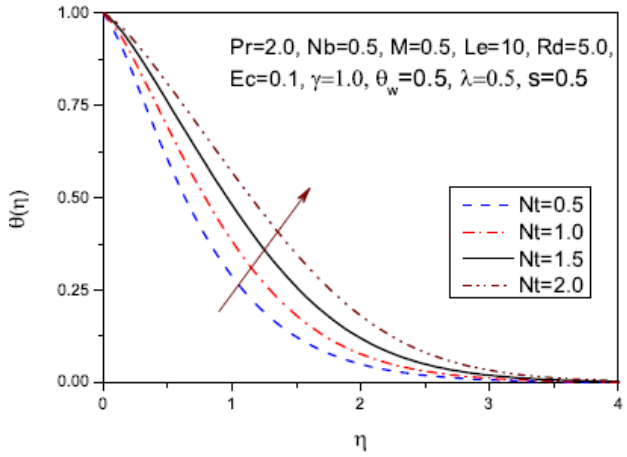

Figure 7: Temperature distribution $\theta(\eta)$ vs. η for different values of Nt.

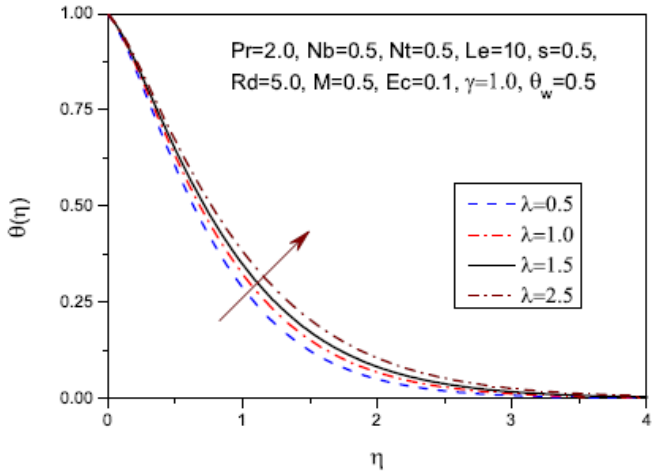

Figure 8: Temperature distribution $\theta(\eta)$ vs. η for different values of λ.

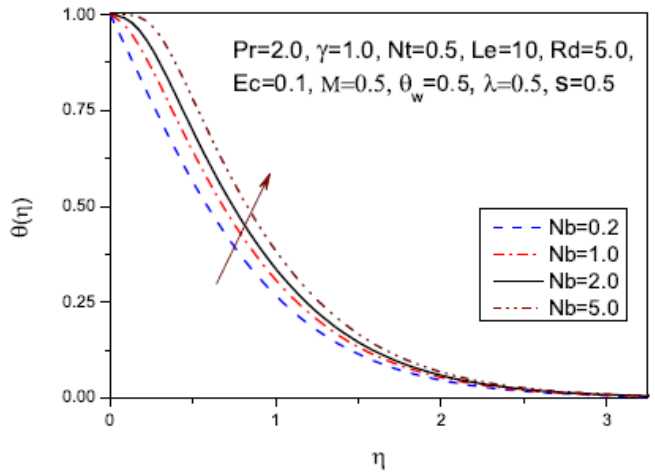

Figure 9: Temperature distribution $\theta(\eta)$ vs. η for different values of Nb.

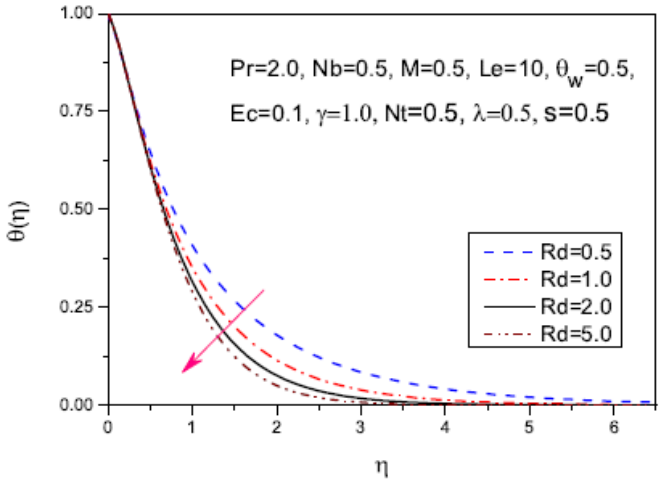

Figure 10: Temperature distribution $\theta(\eta)$ vs. η for different values of Rd.

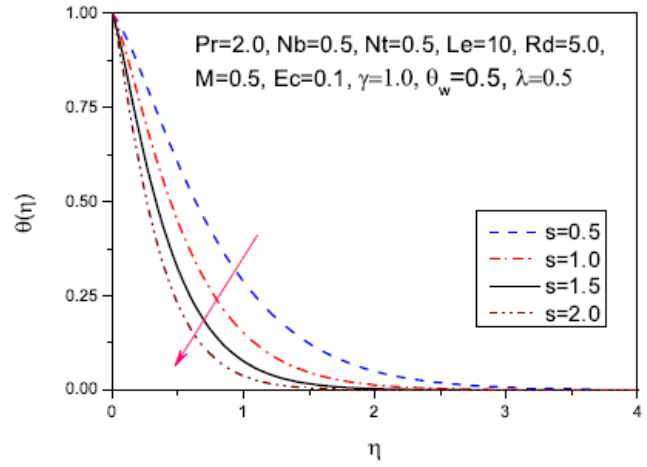

Figure 11: Temperature distribution $\theta(\eta)$ vs. η for different values of s.

Figs. 12 & 13 display the variation of the distribution of Casson nanoparticle concentration $\phi(\eta)$ vs. η for several values of the suction parameter s and the Lewis number Le respectively. From figs. 12 & 13, it is observed that the Casson nanoparticle concentration falls with an augmentation in the value of the suction parameter and the Lewis number. It is concluded that the effect of the Lewis number on the Casson nanoparticle concentration is very forceful which is effective only in a field near to the stretching surface as the tendency of the profiles are to meet at greater distance from the stretching sheet till its value gradually diminishes. Fig. 15 & 16

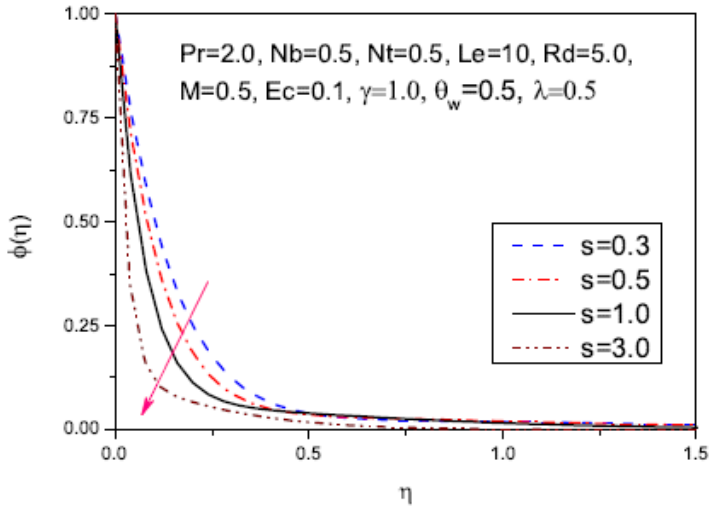

Figure 12: Variation of nanoparticle volume fraction $\phi(\eta)$ vs. η for different values of s.

depict the variation of the Nusselt number $Nu_x/Re_x^{1/2}$ and the thermophoresis parameter Nt with the suction parameter s and the slip factor parameter λ respectively. It is found that the Nusselt number decreases with an increase in the value of Nt and λ but the opposite trend is seen for s. Further, figs. 17, & 18 show the variation of the Sherwood number and Lewis number Le for several values of the slip factor λ and the suction parameter s, respectively. It is noted that the Sherwood number increases with an increment in the value of s and Le whereas reverse effect is seen with the augmentation of slip factor for all the values of Le and s.

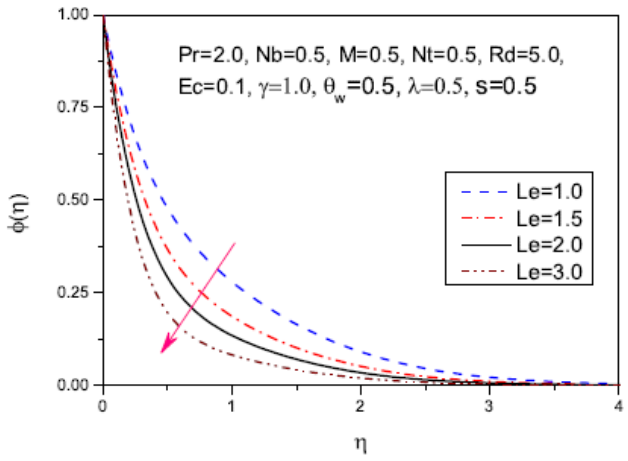

Figure 13: Variation of nanoparticle volume fraction $\phi(\eta)$ vs. η for different values of Le.

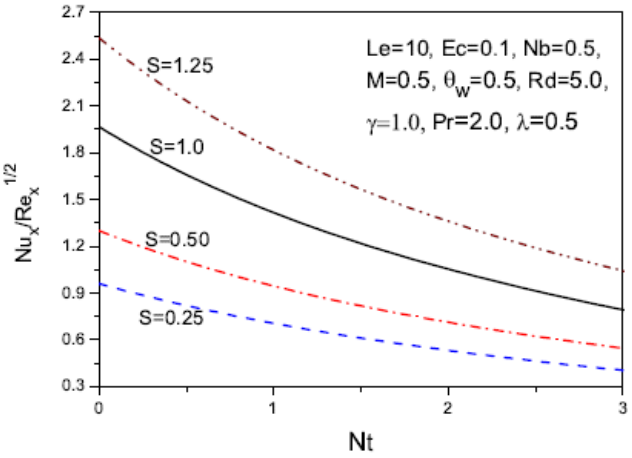

Figure 14: Effect of s and Nt on Nusselt number.

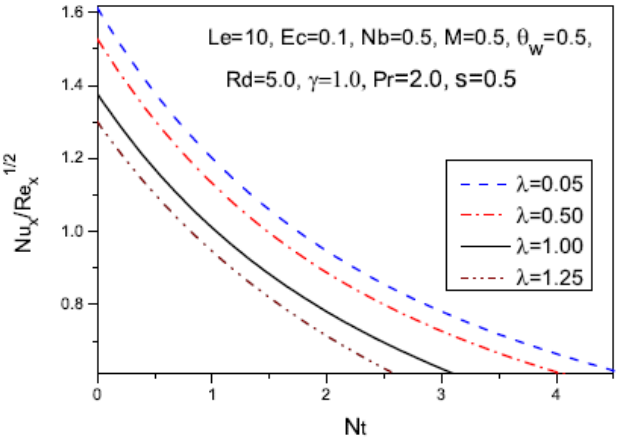

Figure 15: Effect of λ and Nt on Nusselt number $Nu_x/Re_x^{1/2}$.

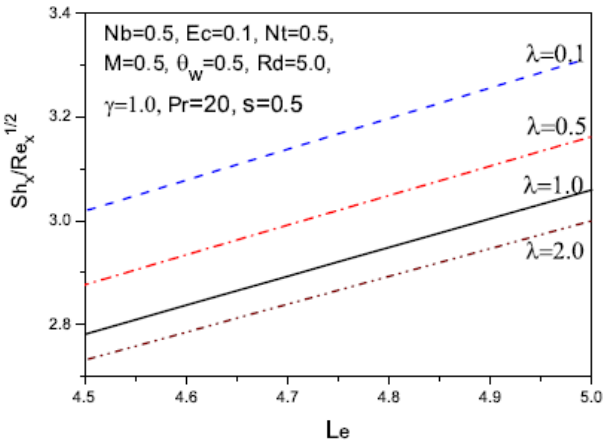

Figure 16: Effect of λ and Le on Sherwood number.

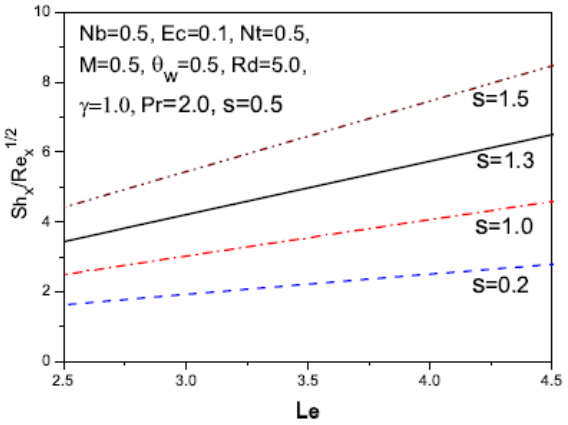

Figure 17: Effect of s and Le on reduced Sherwood number.

5. Conclusion

In the present study, the effects of non-linear thermal radiation and the magnetic field on the boundary layer flow and heat transfer of Casson nanofluid over a stretching surface in the presence of the Ohmic dissipation are explored. In order to obtain a set of non-linear ordinary differential equations in this work we employed the similarity transformation on the boundary layer basic equations and solved them numerically on the physical parameters of suitable combinations of Casson nanofluid. Following conclusions are derived from the present study:

(i) Velocity profile $f'(\eta)$ decreases with a rise in the Casson parameter γ, suction parameter s, the slip parameter λ and the magnetic parameter M near the stretching sheet.
(ii) In the thermal boundary layer, the temperature profile $\theta(\eta)$ enhances with the augmentation in the value of the magnetic parameter M, the slip parameters λ, the thermophoretic parameter Nt, wall temperature excess ratio parameter θ_w, Casson parameter γ, but the opposite tendency is seen in the value of the radiation parameter Rd, the suction parameter s and the Prandtl number Pr.
(iii) Casson nanoparticle volume fraction near the stretching surface falls with an increment in the Lewis number Le and the suction parameter s, the Brownian motion parameter Nb and the reverse trend is seen in the value of the thermophoretic parameter Nt.
(iv) The advancement in local Nusselt number is obtained with rise in s but opposite fact is observed by enhancing γ, M, Nb, Nt, λ and θ_w.
(v) The local Sherwood number enhances with increasing s, Nt, θ_w, Nb but reverse trend is noticed by rising γ, M, λ, Ec, Rd.

Reference

[1] J. Buongiorno, Convective transport in nanofluids, ASME J. Heat Transfer 128 (2006) 240-250.
[2] S. U. S. Choi, Enhancing thermal conductivity of fluids with nanoparticles, in: The Proceedings of the 1995 ASME International Mechanical Engineering Congress and Exposition, San Francisco, USA, ASME, FED 231/MD 66 (1995) pp. 99-105.
[3] D. A. Nield, A. V. Kuznetsov, The Cheng-Minkowycz problem for natural convective boundary layer flow in a porous medium saturated by a nanofluid, Int. J. Heat Mass Transfer 52 (2009) 5792-5795.
[4] Makinde OD, Aziz A. Boundary layer flow of a nano fluid past a stretching sheet with a convective boundary condition, Int. J. Therm. Sci. 53(11) (2011) 2477-83.
[5] D. Pal, N. Roy, Influence of Brownian motion and thermal radiation on heat transfer of a nanofluid over stretching sheet with slip velocity, Int. J. Appl. Comput. Math. 3(4) (2017) 3355-3377.
[6] S. Mukhopadhyay, Effects of thermal radiation on Casson fluid flow and heat transfer over an unsteady stretching surface subjected to suction/blowing, Chin. Phys. B. 22(11) (2013) 114702.
[7] S. Pramanik, Casson fluid flow and heat transfer past an exponentially porous stretching sheet in presence of thermal radiation, Ain Shams Eng. J. 5 (2014) 205-212.
[13] D. Pal, N. Roy, K. Vajravelu, Effects of thermal radiation and Ohmic dissipation on MHD Casson nanofluid flow over a vertical non-linear stretching surface using scaling group transformation, Int. J. Mech. Sci. 114 (2016) 257-267.

[9] G. Sarojamma, K. Vendabai, Boundary layer flow of a Casson nanofluid past a vertical exponentially stretching cylinder in the presence of a transverse magnetic field with internal heat generation/absorption, Int. J. Mech. Aerosp. Ind. Mechatr. Eng. 9 (1) (2015) 138-141.
[10] K. Bhattacharyya, MHD Stagnation-Point Flow of Casson Fluid and Heat Transfer over a Stretching Sheet with Thermal Radiation, J.Thermodynamics 2013 (2013) Article ID 169674.
[11] I. S. Oyelakin, S. Mondal, P. Sibanda, Unsteady Casson nanofluid flow over a stretching sheet with thermal radiation, convective and slip boundary conditions, Alexan. Eng. J. 55 (2016) 1025-1035.
[12] S. Mukhopadhyay, K. Vajravelu, Van Gorder R A. Casson fluid flow and heat transfer at an exponentially stretching permeable surface, J. Appl. Mechanics, 80 (2013) 054502.
[13] D. Pal, N. Roy, Lie group transformation on MHD radiative dissipative Casson nanofluid flow over a vertical non-linear stretching surface with non-uniform heat source/sink and chemical reaction, J. Nanofluids. 5(6) (2016) 839-851.
[14] D. Pal, N. Roy, Role of Brownian motion and nonlinear thermal radiation on heat transfer of a Casson nanofluid over stretching sheet with slip velocity and non-uniform heat source/sink, J. Nanofluids. 8(3) (2019) 556-568.
[15] R. Kandasamy, P. Loganathanb, P. Puvi Arasub, Scaling group transformation for MHD boundary-layer flow of a nanofluid past a vertical stretching surface in the presence of suction/injection, Nucl. Eng. Design. 241 (2011) 2053-2059.
[16] C.Y. Wang, Free convection on a vertical stretching surface. ZAMM. 69 (1989) 418-420.
[17] R. S. R. Gorla, I. Sidawi, Free convection on a vertical stretching surface with suction and blowing. Appl. Sci. Res. 52 (1994) 247-257.

Netai Roy, et. al. "Role of Magnetic Field with Nonlinear Thermal Radiation and Ohmicdissipation of a Casson Nanofluid over Stretching Sheet Considering Slip Velocity." *International Journal of Engineering Science Invention (IJESI)*, Vol. 09(09), 2020, PP 49-55. Journal DOI- 10.35629/6734